AIMS Geosciences

AIMS Geosciences, 5(2): 163–183.
DOI: 10.3934/geosci.2019.2.163
Received: 20 February 2019
Accepted: 29 April 2019
Published: 20 May 2019

http://www.aimspress.com/journal/geosciences

*Case report*

# Bryozoan limestone experience—the case of Stevns Klint

**Nataša Katić*, Joakim S. Korshøj and Helle F. Christensen**

Geo, Maglebjergvej 1, 2800 Kgs. Lyngby, Denmark

*** Correspondence:** Email: nka@geo.dk; Tel: +4545204275.

**Abstract:** Bryozoan limestone is a formation of Danian limestone, generally found underlying the younger Copenhagen formation and above the Cretaceous chalk. The mineralogy between the Danian and Cretaceous formations is similar, resulting in similar mechanical responses of the matrix material. The mineralogy of the mentioned formations generally includes calcareous minerals with variable contents of flint (siliceous materials) and irregularly a small content of other materials. The distinctive feature of the matrix material of these formations is primarily the type of porosity reflecting the originating organisms and depositional history. Our database includes Bryozoan limestone data collected on major infrastructure projects between Sjælland (Denmark) and Skåne (Sweden), such as Malmø Citytunnel, as well as from a number of smaller investigation campaigns. The database includes borehole registrations, geological descriptions, classification tests and basic strength tests. Further knowledge collection includes results of wireline logging, advanced laboratory tests etc. In the latest campaign on the Bryozoan limestone, the site and material are investigated for the design of the rock anchors at the UNESCO site of Stevns Klint. The article presents a part of the interpretation of the mechanical behavior of Bryozoan limestone aided by the use of the existing database.

**Keywords:** Bryozoan limestone; Stevns Klint

## 1. Introduction

Bryozoan limestone, also known as the Stevns Klint formation, is a formation of Danian limestone, generally found underlying the younger Copenhagen formation and above the Cretaceous chalk. The mineralogy between the Danian formations and Cretaceous chalk is comparable, thereby resulting in similar mechanical responses of the matrix material.

Reviews of the geotechnical experience with Danian limestone up to 2010 have been presented by Jackson et al. [1] and Foged [2] and Foged et al. [3]. Further experiences with Danian limestone gathered on the Cityringen project have been described, inter alia, by Galsgaard [4], Jacobsen et al. [5], Hansen et al. [6], including our contributions [7,8]. However, the vast majority of the works west-southwest of Øresund, concern the Danian limestone of unknown formation or limestone from the Copenhagen formation.

Locations where the Bryozoan limestone is found (and documented) propagate southwest from Malmø and Limhamn quarry across Øresund Link towards Sjælland where it is found at Karlstrup quarry and near Køge, as well as further south in the Fakse quary. The formation is also encountered in Jutland on Karlsby Klint, Sangstrup Klint, Mønsted and Bulbjerg, see e.g. the geological profiles across Denmark suggested by Vangkilde-Pedersen et al. [9].

The development of infrastructure in recent years has provided further information about the Bryozoan deposits on some of the Sjælland locations, albeit generally to a smaller extent. Recently, Geo has been awarded a rare opportunity to investigate the UNESCO site of Stevns Klint and the Bryozoan limestone the formation is named after. At the location, the Bryozoan mounds are found under a few meters of clayey till, above the Cretaceous chalk, overlying Lower Danian Cerithium limestone and occasionally Fish-clay. The rock is investigated for the possibilities of anchoring of a light construction into the cliff.

The goal of the present work is to give an overview of the available experience in terms of the essential geotechnical parameters focusing on Bryozoan limestone.

The data is collected from investigations for the major infrastructure projects between Skåne (SE) and Sjælland (DK) such as Malmø Citytunnel. The database, which includes a variety of in situ and laboratory tests, is presented herein to the extent of interest for the Stevns Klint case study, focusing on the basic properties of the rock material.

## 2. Location and geology of Bryozoan limestone

### *2.1. General*

In early Danian (Palaeogene), cool-water Bryozoan mounds were formed in the Danish Basin, shortly after the Cretasious-Palaeogene mass extinction. The subsequent Bryozoan limestone represents a relative deep-water eco-system with a high diversity along the epeiric seaway that covered the Danish Basin.

The Bryozoans grew in mounds along the paleocurrent. Several generations of Bryozoans make each mound. The Bryozoan mounds are 50–110 m long and reached a height of 5–10 m above the seafloor [10]. Due to the growth along paleocurrent, the mounds are typically asymmetric resulting with the higher frequency of visible flint beds on the sides facing the current.

The Bryozoan limestone is well known from borings and outcrops in Denmark. It is generally found parallel to, and bounded by, the Sorgenfrei-Tornquist zone on the north-east. On the south-west, the limit of its extent reaches the Ringkøbing-Fyn High [10].

Figure 1 shows the position of two general cross sections across Sjælland, in reference to the bounds stated by Japsen et al. [11].

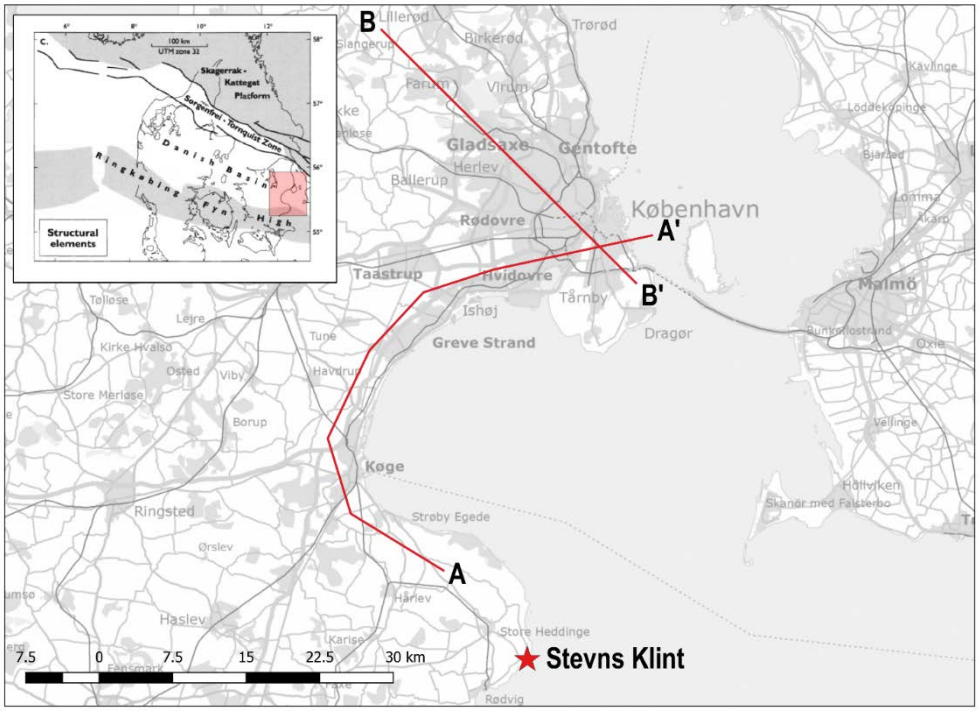


**Figure 1.** Location map.

Figure 2 shows the longitudinal profiles of the lines A-A’ and B-B’ cf. Figure 1. modelled using GeoAtlas Live version 1.2 cf. [12]. The line A-A is depicting the path between the Malmø and Stevns Klint, and the line B-B’ is roughly parallel to the Sorgenfrei-Tornquist zone. The lines A-A’ and B-B’ are crossing the areas where the available information allows the distinction of the Bryozoan limestone within the overall Danian limestone data in GeoAtlas Live database version 1.1.0.

Another distinctive structural feature encountered on the depicted lines is Carlsberg fault (see the right side of the line A-A’ on Figure 2 Several smaller faults are also encountered along A-A’ line.

Towards the end of the Danian a regression took place and in the Copenhagen area the Copenhagen limestone formation is still preserved. The Lellinge greensand formation was deposited in shallower water and overlies the Copenhagen limestone formation (Figure 2).

Based on geophysical logging in the Copenhagen area, Olsen and Nielsen [13] defined the boundary between the Cretaceous chalk and Bryozoan limestone. This boundary is observed through a transition of very smooth resistivity, induction and porosity log patterns in chalk to very unsteady logs in Bryozoan limestone, noting that a peak in gamma log is irregularly appearing. Further markers of the boundary are observed in the underlying chalk.

Where the Copenhagen limestone is encountered overlying the Bryozoan limestone, the boundary is typically not obvious. One of the reasons lays in the similar diagenesis of Lower Copenhagen limestone, involving also bryozoan organisms. The other reasons may include disturbance and re-sedimentation due to e.g. the movements in fault zones.

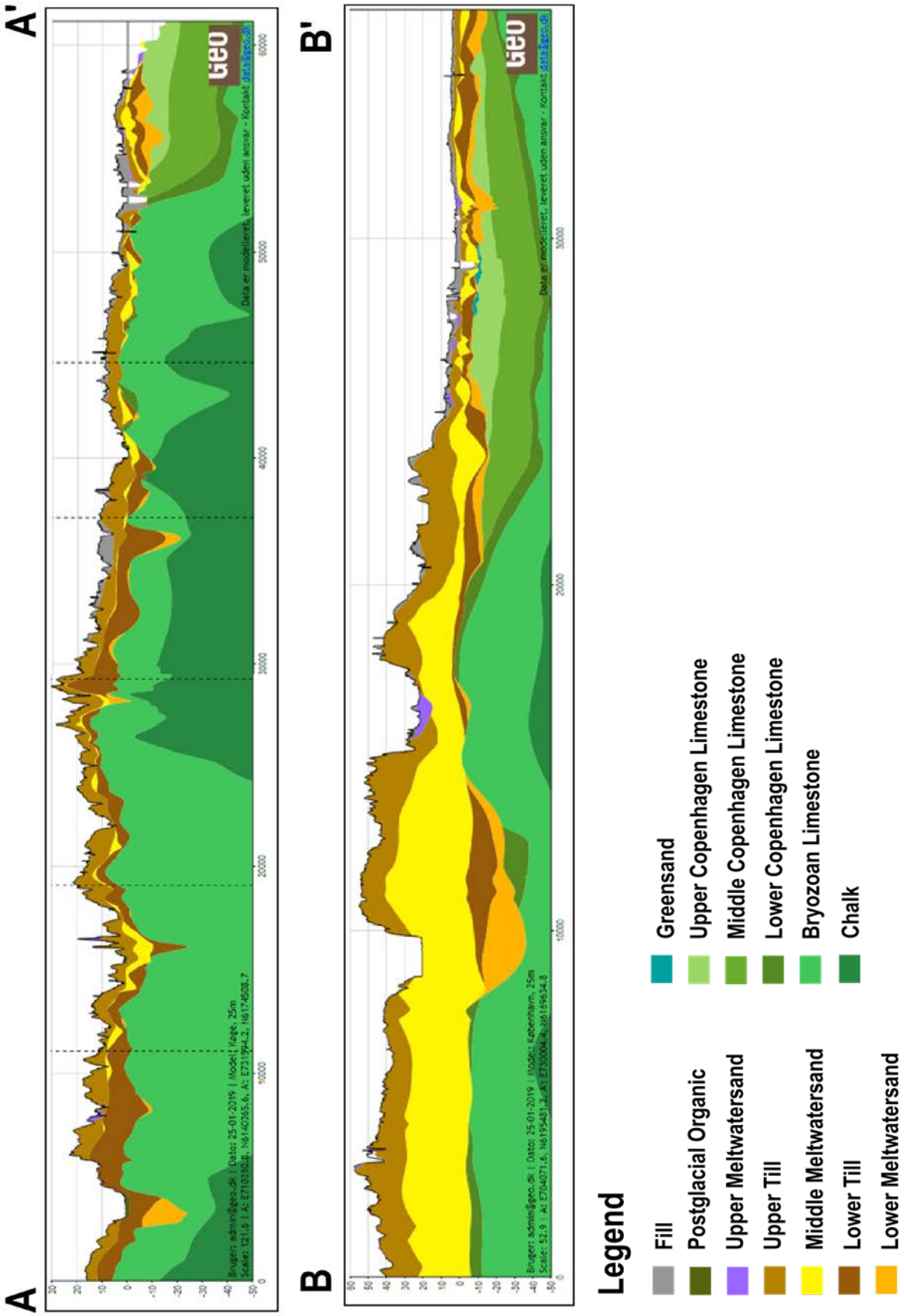


**Figure 2.** Longitudinal profiles A-A' and B-B'. GeoAtlas Live model.

### *2.2. Stevns Klint*

Stevns Klint is a 15 km long scenic coastal cliff positioned about 75 km along the coast south of Copenhagen, see Figure 1 and Damholt and Surlyk, [14]. It documents the global mass extinction event in the history of Earth known as the Cretaceous—Palaeogene boundary, for which it has been inscribed into the UNESCO list of natural sites in 2014.

The general geological profile at the site below Stevns Lighthouse (Figure 3) includes a sequence of rock and soil deposits from Cretaceous (Maastrichtian) chalk at the bottom of the cliff, to Quaternary and recent deposits found at the top of the profile. The chalk is at some places overlain by Fish clay, and everywhere by a thin layer of Cerithium limestone. Above the Cerithium limestone lie the mounds of Bryozoan limestone consisting of alternating thick layers of white carbonate rock and thin layers of dark flint. The thickness of the Bryozoan formation on the site is about 20 m.

### *2.3. Bryozoan limestone material*

The constituents of the Bryozoan Limestone are the carbonate matrix, the carbonate skeletons and shell debris, the carbonate cement, quartz and associated components (clay minerals, pyrite etc.). Jørgensen [16] showed that the non-carbonate components play only a limited role for the structure of the sediment. The Bryozoan limestone consists predominantly of grains in the silt fraction (average 30 μm) and is thus considerably coarser than most chalk formations. The coarseness is caused by invertebrate skeletal components (10–25 wt%), dominated by Bryozoans in the fraction > 75 μm, with randomly oriented grains. The amount of non-carbonate content in samples from Jutland is quite constant ranging within 4–8 wt%. This range corresponds to the Rock type 1 [1], with the carbonate content exceeding 90% and grain density exceeding 2.65 g/cm$^3$, typically 2.7 g/cm$^3$.

Galsgaard [4] states that 95.6% of the flint in Bryozoan limestone belongs to the light limestone, described as “sandy, muddy, almost clay-free, very light grey to slightly clayey light grey limestone with bioturbations”. The remaining 4.4% of the flint belongs to the dark limestone—or “visual flint” as called in Malmø Citytunnel project—described as “bedded, slightly clayey medium light grey to clayey grey limestone, with clay laminae and bioturbations, and rare clay layers up to a few cm”. According to the Citytunnel documentation [15], the amount of visual flint in the Bryozoan deposits of Malmø is low (0–3%) in comparison with the visual flint in Copenhagen limestone.

A correlation between the low carbonate contents and low densities of the solid particles found on Malmø specimens indicated that the insoluble part of the tested limestone mainly consists of white opal flint, in the range of 10–20%.

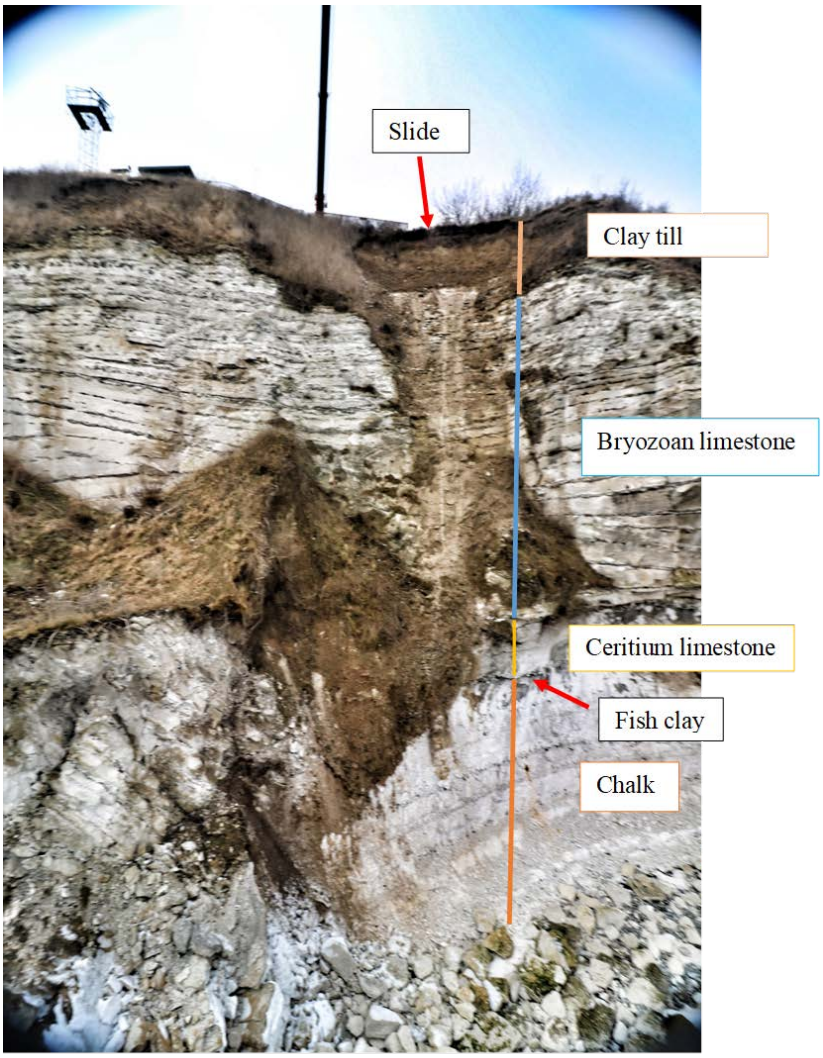


**Figure 3.** Cliff below Stevns Lighthouse.

## 3. Stevns Klint investigations and large scale observations

### *3.1. General*

Rosenbom and Jakobsen [17] have measured fracture density at the Sigerslev quarry not far from the Stevns Klint. They have found that dominant fracture orientation is north-northeast—south-southwest and observed that the top six meters of limestone is generally closely fractured. They concluded that the fractures originate from the pressure applied during ice load from glaciers during the Quaternary period. The area of Stevns Klint has experienced uplift of about 600 m by combined late Cretasious and Cenozoic basin inversion and regional Neogene uplift, and the succession was originally buried beneath Cenozoic deposits, which now has been eroded, see Surlyk et al. [18].

Having been of immense geological importance, the site has been thoroughly geologically researched for more than 200 years [14]. However, geotechnical information about the area is very limited. Preceding the current project, the total geotechnical information for the area at a distance of

100 m from the cliffside on either side of Stevns Fyr (Stevns Lighthouse) included one boring with geological descriptions. The closest borings reaching the Bryozoan limestone are more than 500 m away from the cliffside, including primarily geological descriptions.

### *3.2. Present investigations*

The currently presented investigations have been done for a preliminary design of the light structure on the cliff face. The details of foundation design and loads were unknown, but rock anchors were anticipated foundation type.

The current investigation focused on the cliffside below Stevns Fyr located at the highest point on the cliff. The top of the cliff is approximately 41 m above sea level. On this cliffside profile, a planned light structure should enable a closer look at the cliff to a wider audience.

The goals of investigation were set to extrapolate, supplement and specify the existing knowledge, gathered generally for large structures, to the local conditions and structures of rather limited extent such as rock anchor heads.

The three stages of the current investigation included:

- Review of historical data, geological inspection, face logging and 3D survey of the cliff and overall risk assessment with respect to the planned construction and in relation to further investigation.
- Drilling of three geotechnical boreholes in Bryozoan limestone, and geophysical borehole logging in two of the boreholes.
- Laboratory investigation and interpretation of all the gathered data.


**Figure 4.** Layout of the present investigations (including boreholes BH4–BH6 and face logging lines 0–5).

Proportionally to the limited size of the structure, the overall budget of the investigation was limited, thus a great attention is payed to observing as many details as possible. The laboratory

measurements are thus carried out on the companion neighbouring specimens obtained from the same samples. Special care is taken to choose the sets of specimens with negligible variation of density between them, in order to enable direct interpretations. More so, the selected samples reflect the weakest portions of the rock (induration H2) in order to enable comparison with the trends observed on the database data (induration H3). Therefore, the obtained dataset has a (planned) bias towards the worst-case scenario concerning local conditions within the rock mass rather than the rock mass as a whole.

### *3.3. Cliffside condition and face logging at Stevns Klint*

The erosion of the cliff potentially affects all the structures at the location. The general mechanism of the cliff erosion has been reviewed by Pedersen in 2011 (cf. Damholt and Surlyk, 2012 [14]). He outlined that the internal framework of the Bryozoan limestone with hardgrounds and mound shaped flint bands increases its resistance to erosion. Pedersen concludes that "the rockfalls at Stevns Klint are solely related to the erosion of the soft chalk situated below the hard Bryozoan limestone with its increased strength due to the strong flint beds.", and the observed overhang portions of the Bryozoan limestone protruding above the beach generally confirm this. The planned structure is thus positioned on the part of the cliffside that has experienced slope failure previously (Figure 3). There, the slithered material is extending from the beach to a level above the Cretaceous-Palaeogene boundary and offering some protection of the underlying chalk from the wind and wave action, thereby increasing the overall stability of the cliff.

Falling debris (Figure 5) increased the difficulty of executing the site investigation. This was particularly important during midday when the sun shining on the cliff for some hours was thawing the frozen cliffside. Smaller landslides of the overlying quaternary deposits and chipping of the smaller blocks of rock occurred in a few places during the investigation.

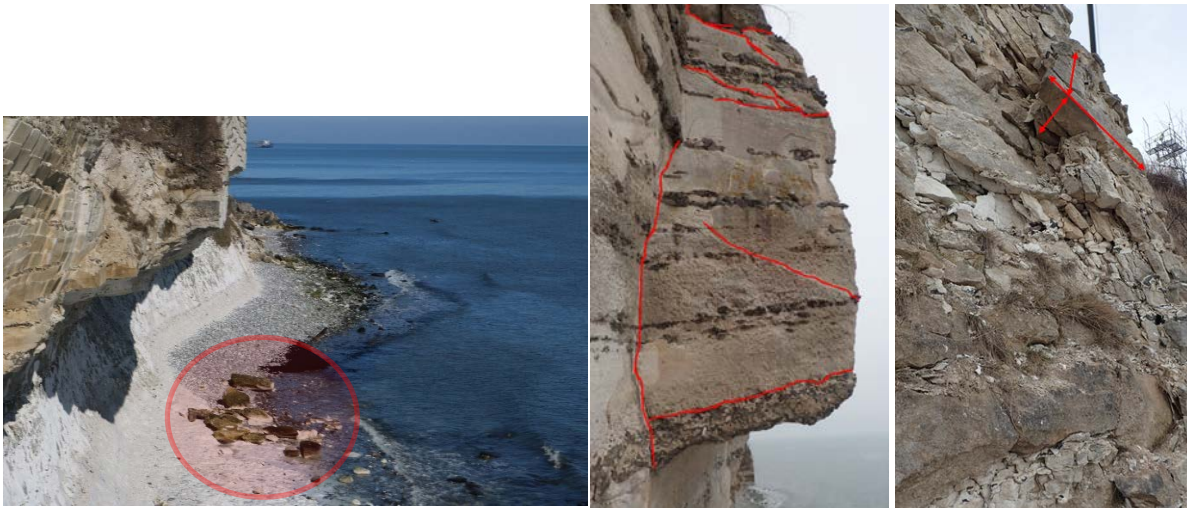

**Figure 5.** Overhang; rock fall and fractures on the slope (outlined with red; block group 40 × 50 × 150 $cm^3$ of about 800 kg). Photo J. Korshøj.

Along the Stevns Klint large blocks of the Bryozoan limestone fall down as the underlying chalk is eroded by wind and wave action. These blocks are of approximately the same size and mostly oriented in the same directions (Figures 3 and 5), which indicates that a system of fractures is relatively uniform. In the face-logged area, fractures of various sizes are seen.

The face logging was carried out from a mobile crane. Due to its load, the crane had to stand 40 m from the edge of the cliff—roughly the distance equal to the height of the cliff—maintaining the ratio of 1:1 for safety reasons. At some points it was difficult to get close enough to the cliff because of the overhang. This affected the measurement of the induration, as the basket could be pushed away from the cliff in case the grip was not sufficiently strong.

This experience illustrated the expected problems with anchoring from the cliffside: the difficulty to approach the setting points and the general safety against local slides during the execution.

**Figure 6.** Face logging. Project photos (J. Korshøj on the right).

Natural water level was not encountered in the boreholes on Stevns Klint. Due to this, some of the geophysical investigations could not have been carried out to the planned extent or at all, e.g. porosity logging.

When exposed to weathering, the surface of the Bryozoan limestone seems to harden, hence faces that have been exposed to weathering for a long time have a higher induration than more freshly exposed Bryozoan limestone. In the opposite manner, the chalk below is quickly eroded by weathering and by wave erosion. This hardening feature of the limestone is in agreement with the indurations logged on the cliff faces and in the boreholes (see the following section), as well as with the observations during the handling of the laboratory samples.

The flint types seen at cores from the current site match the flint seen in the cores from the Bryozoan limestone found in Copenhagen area. Even though fewer Bryozoan fossils are visible in the cores from Copenhagen in comparison with the cores from Stevns Klint, it is hard to make a distinction based on the images of the cores. Cores from Copenhagen tend to show more silicified or strongly indurated parts than seen at the Stevns Klint cores.

### *3.4. The state of the Bryozoan limestone at Stevns Klint*

The rock at Stevns Klint is famous for its layered appearance (see the Figures 3–6) with alternating layers of black flint and white carbonate material. As an essential description, the induration of the rock is logged in accordance to Danish practice.

Based on the observations from the borehole logs, the thickness of the dark flint beds ranges from 5 to 30 cm. Parallel observations on cliffside photographs and optical televiewer logs show that the flint beds repeat with the spacing of about 0.5 m, but also reveal the discontinuity and variation of the flint bed thicknesses. This is illustrated in Figure 7a where a part of the optical televiewer log of one of the boreholes is overlaid with the corresponding H5 induration logged on the retrieved cores.

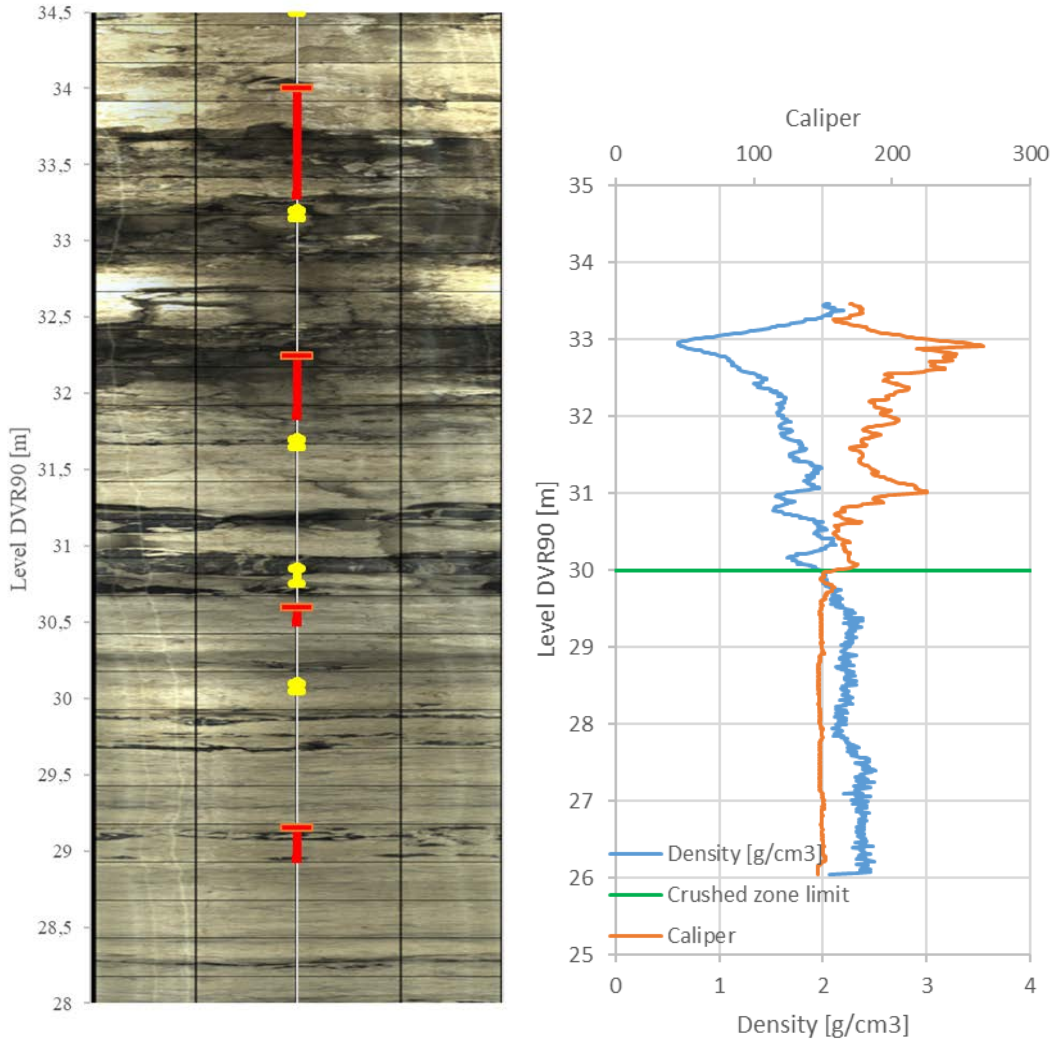


(A) (B)

**Figure 7. A**: Optical televiewer log (part). Yellow: induration H5; Red: core loss)
**B**: Geophysical log (selection).

The percentage of H5 induration varies between the logs. This is partly a consequence of variation of the H5 concentration along the depth of the rock vs. the difference in lengths between the borehole logs and the face logs, and partly a consequence of the mentioned core loss during drilling of the boreholes illustrated in Figure 7b.

The induration is logged over the total lengths of the profiles, with averaging over 5 cm both in the boreholes and on the cliffside faces. The results of the induration logging are presented in Figure 8. Discrepancies between the frequency of H5 induration (dark flint) observed on the cores and based on the televiewer partly stem from the discontinuities in the flint beds, but may also arise from the coring process, where the alternation of stiff and soft layers could result in core loss.

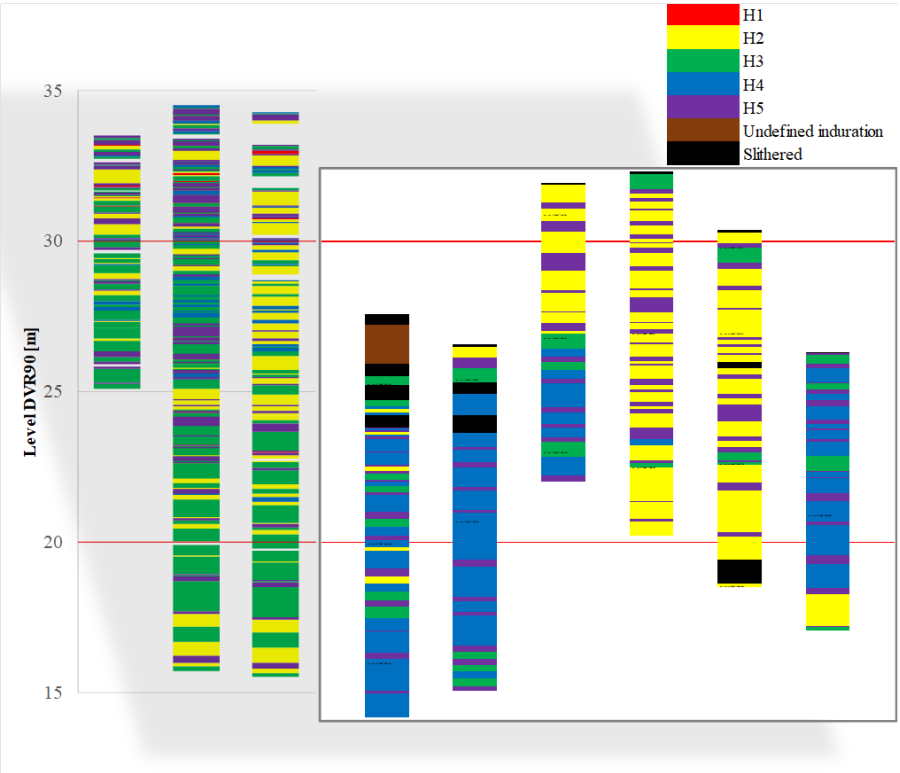


**Figure 8.** Induration logs (boreholes on the left and cliff faces in the square on the right).

Based on the differences between the indurations recorded on the cores and on the face logs, lower indurations are recorded on the portion of the cliffside which experienced more recent slide (the yellow-dominated profiles on the right side of Figure 8). The average induration of the rock on these profiles is a consequence of the absolute position and shorter length of the face logs in comparison to the borehole logs. However, Figure 8 shows that the lower portions of the borehole profiles are not as indurated as the rock on the matching levels of the cliffside, which is the consequence of hardening of the exposed surfaces due to weather.

The lower sections of the rock seem generally more indurated than the upper sections, which is also confirmed by geophysical logging (Figure 7, right side), where an abrupt increase of the formation density on the presented log is marking the change towards the higher induration. Such variation is not observed on the other side of the planned construction site. Based on this and on the variation of indurations, forming “discrete zones with quite clearly different characteristics” [1], it

may be stipulated that these differences originate from different mounds on opposite sides of the site, Supporting this is also the observed variation of the mounds just above the slithered portion of the rock presented in Figure 3.

Ultimately, it is worth noting that the ranges of recorded indurations on the face logs where the profile has undergone hardening are in agreement with the upper bound distribution of indurations obtained in the Malmø Citytunnel project. In other face logs and boreholes, a concentration of weaker indurations is apparent.

If the general inclination of the Bryozoan mounds in the direction of paleocurrent is added to the observations, and accounting for the differences caused by local erosion, it can be concluded that any statistics on induration of the rock based on the borehole logs requires, as a minimum, a confirmation by visual observations through face logging and/or optical televiewers. This further emphasizes the importance of combining geological observations with engineering judgement.

The above conclusion naturally extends to the analysis of fractures. At the present site, the upper crushed zone identified based on the borehole logs and geophysical logging, including the televiewer logs (Figure 7) is found in the top 4 m. The variation between the RQD evaluated on the face logs and on the cores is about 3 to 5 times, showing the effect of the coring process. This variation is larger in the upper zone. From the lower, fairly intact, zones of the rock, large pieces of core without fractures are retrieved. Thus in the lower part of the rock, the RQD based on the optical televiewer, face logging and cores scatters less.

The propagation of the crushed zone behind the cliffside varies depending on the level, as well as the time lapse from the most recent collapse. In both of these zones, variable low GSI values [19] are estimated. On the contrary, the remainder of the rock is in a fairly intact state with GSI values generally in excess of 70.

## 4. Results of laboratory investigations and interpretations

### *4.1. Build-up and classification of limestone matrix*

In order to get an idea about the mechanism through which the rock has obtained its strength, the p-wave velocities measured on specimens for testing the unconfined compressive strength (UCS) are plotted versus the porosity in Figure 9. The data from Stevns Klint are plotted together with the laboratory data from the Malmø Citytunnel and the Copenhagen limestone data gathered primarily on Cityringen project (cf. [8]).

Rules of mixtures provide theoretical bounds for the stiffness of composite materials [8]. Voigt and Reuss bounds relate to axial and transversal loading, thereby defining the uppermost and the lowermost bounds presented in Figure 8, respectively. Following Eberli et al. [20], Katić & Christensen [8] and Brigaud et al. [21], the anticipated trends of data for processes involving cementation with and without initial compaction are sketched in Figure 9. The laboratory data, plotting above the trend for compacted mud [20], indicates that the development of rock strength of the Danian limestone, and especially of the Bryozoan limestone, is dominated by cementation process. The lower bound (Reus vp line in Figure 9) p-wave measurement from Malmø indicates remoulded carbonate material. Ultimately, it is worth mentioning that the registered porosity of the matrix material on the site varies between 20 and 40%, while the testing was only conducted on the samples with a porosity between 30 and 40%.

During the laboratory work on the samples obtained from the current boreholes, the weakness or occasional complete lack of cementation was easy to observe, along with chipping of the well preserved Bryozoan fossils. This is in line with the overall description by Jørgensen et al. [15] and observations of Bjerager and Surlyk [10] that "the lack of the framework buildup and the poorly cemented nature of the mounds of Stevns Klint is remarkable".

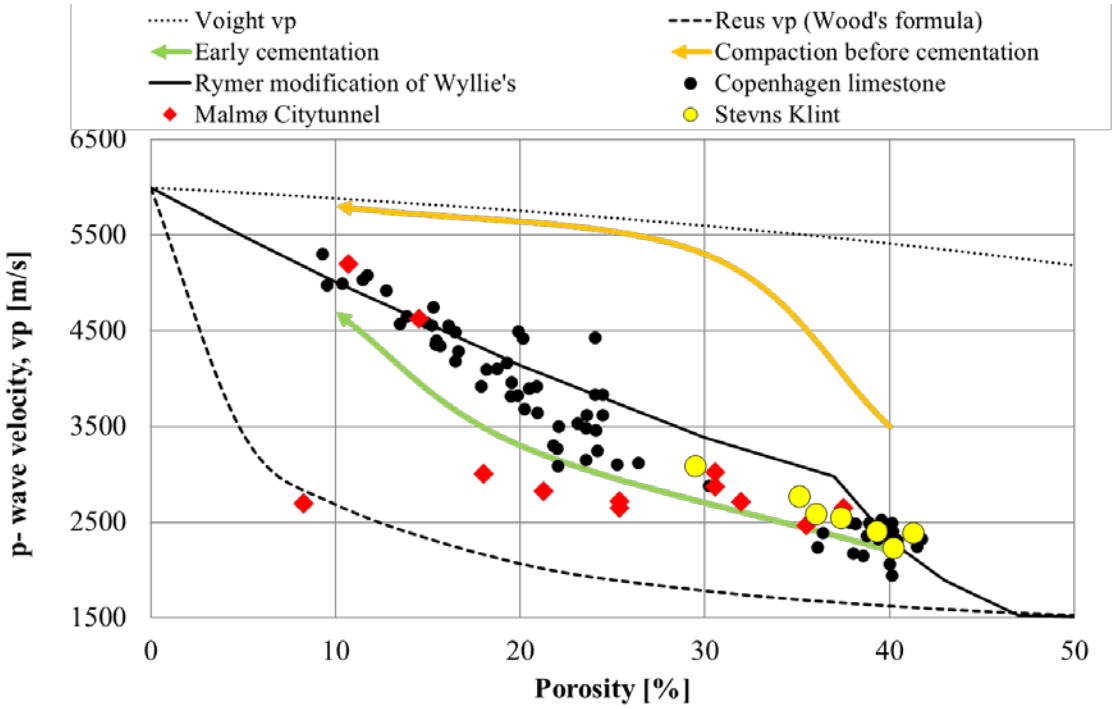


**Figure 9.** P-wave velocity vs. porosity.

The carbonate content measured on the UCS test specimens varies in the range of 92 to 98%, and the variation of the particle density is between 2.70 and 2.72, confirming the similarities with Rock type 1 [1]. The observed variations have a negligible influence on the modeled bounds presented in Figure 9. It can be assumed that the actual content of opal and carbonate phase minerals (aragonite vs. calcite) in the Stevns Klint samples may only have a minor influence on the mechanical properties.

All the classification parameters are found to fit well within bounds of database data.

### *4.2. Mechanical properties of rock elements*

Initially, a short series of Point Load index tests was carried out on lump specimens of induration H2, before and after subjecting them to saturation and 5 cycles of freezing and thawing, each lasting for a minimum of 12 hours. The testing revealed that the fractured surfaces, upon splitting by the Point Load test, typically have somewhat lower induration than the original lumps. This was observed both in the initial lumps split at natural moisture content, and in the saturated samples after the freeze-thaw cycles. This is congruent with the hardening due to elements exposure

observed on cliffside face logging. The 50 percentile value of the Point Load index, both before and after the freeze-thaw cycles, of 0.28 matched the value for H2 induration found in the Citytunnel project. The mass of the samples also did not show a significant variation. However, in light of the short series (12 tests and 5 cycles), these results are considered to be descriptive rather than determinative.

Following the approach of Jackson et al. [1], the uniaxial compressive strengths (UCS) and tensile strengths measured by means of indirect tensile test (Brazil test) are compared with bulk and dry densities. The most robust trends of local data are observed in relation to the intact dry density shown in Figure 10.

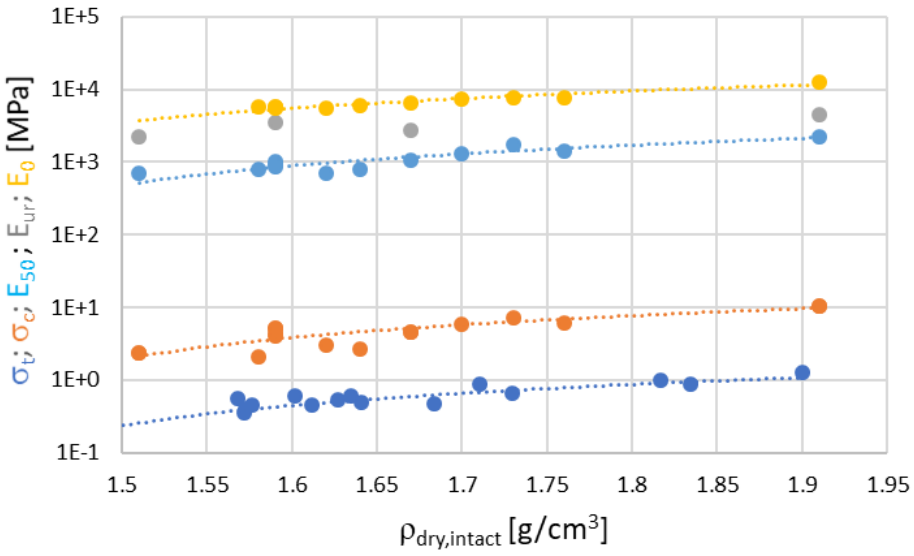


**Figure 10.** Intact rock element strength and stiffness on Stevns Klint.

Worth noting is that Brazil testing in two orthogonal directions, parallel to the coring and orthogonal to the coring direction, has not confirmed anisotropy of the matrix, even though this was assumed based on visual inspection of the samples.

The Figure 10 illustrated proportionality between various strength and stiffness parameters including the results of the stiffness measurements including elastic modulus at 50% of failure stress $E_{50}$, unload-reload modulus $E_{ur}$, and small strain elastic modulus $E_0$ based on acoustic velocities obtained using piezo-crystals. For the current dataset the ratio, $E_0/\sigma_c$ generally exceeds 1000.

The trends of strength in comparison with the overall database data are presented on Figure 11.

Taking into account that the dataset for Stevns is strongly biased towards the weakest portion of the rock, it can be observed that the data follows the anticipated trend of Rock type 1 [1], as expected based on the results of the carbonate content measurements.

The failure strain in UCS tests is generally found to be about twice the strain at 50% to failure, indicating a brittle elastic response prior to failure under unconfined conditions. The degradation of the elastic modulus at 50% of failure strain, which is generally about 0.25%, is likely to be in a range of 0.15 to 0.2, higher for the specimens with higher density. This is in agreement with our experiences with Copenhagen Limestone [7].

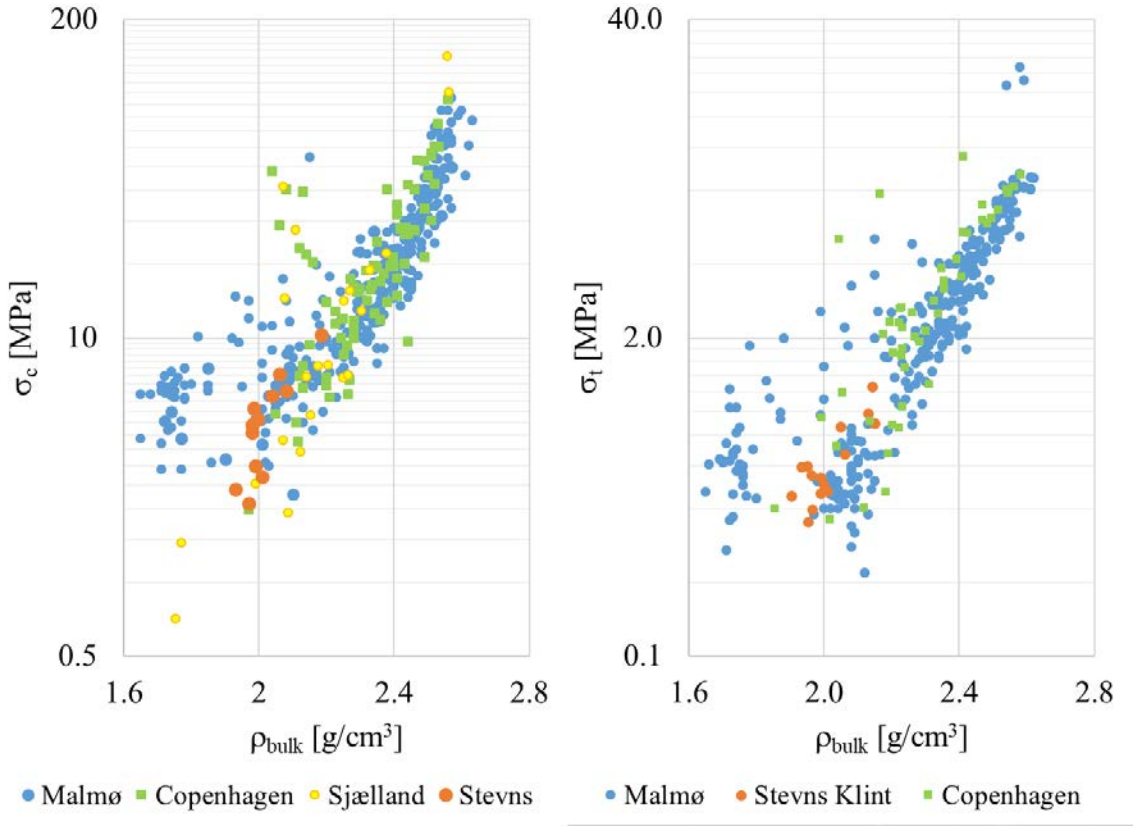


**Figure 11.** Overview of Unconfined compression strength and indirect tensile (Brazil) strength of Bryozoan limestone.

### *4.3. Engineering properties of the matrix material*

It can be observed that the ratio between the unconfined compressive and tensile strengths generally varies between 7 and 10, lower for the lower bulk or dry density, and higher for the samples with higher induration. This range shows a rock matrix angle of friction in excess of 45° with an effective cohesion c in excess of 100 kPa, as expected for intact matrix strengths, see Figure 12. The stated friction angle and cohesion refer to the rock mass rather than to the matrix, but according to [1], the friction angle is largely unaffected by the scale, whereas the effect of the scale is mostly reflected on the cohesion.

As the structure is to be affected by the wind, information about the cyclic resilience under frequencies typically applied for offshore structures was requested. However, at present, there is no reference model for the cyclic strength of Danian limestone at these frequencies. Bergdahl & Steenfelt [22] reported that the strength of Danian limestone is largely unaffected by cyclic pre-shear. The tests [22] were carried out in a large triaxial cell with about 20 cycles per hour on 0.5 m high samples of H/D ratio 1:1 with various stress ratios.

In order to check that this database information is suitable for a small structure, such as an anchor head, it is considered that a small structure may not engage the response from a combination of indurations and may be embedded in the weakest rock matrix detached from the mass by a system of fractures. Due to this, the confinement conditions for the anchor head may not exceed the in situ stresses, and influence of preconsolidation is expected to be minimal.

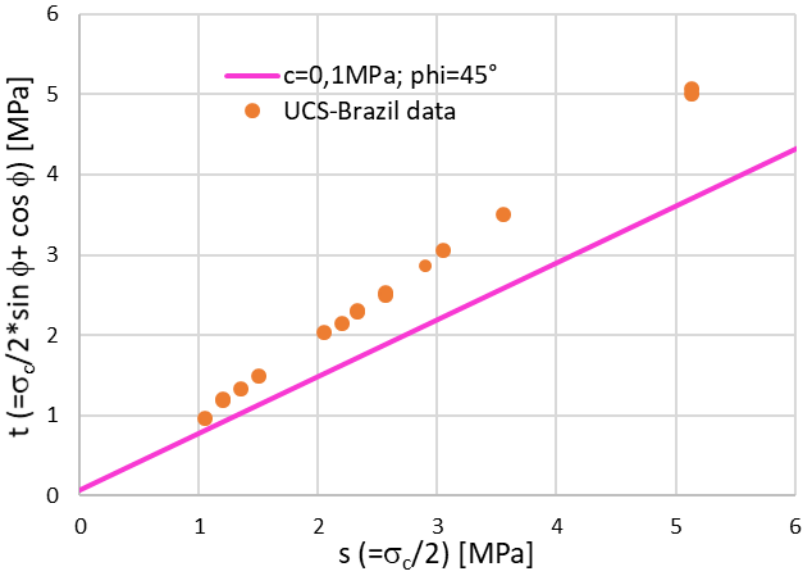


**Figure 12.** Intact strength in s-t space.

Finally, it has been decided to carry out two small scale laboratory cyclic tests. As the strength of the Bryozoan limestone is at least an order of magnitude higher than the strengths of soils typically tested in cyclic DSS, two cyclic triaxial tests have been planned and performed. The overall plan for the two cyclic tests of the current investigation was to include cyclic pre-shear, and a monotonic post-cyclic phase. The aim was to observe the variation of the strength, thus mimicking the overall meso-scale tests from the database, but under limited confinement and at a higher frequency.

The cyclic triaxial tests have been carried out on standard 15 cm tall specimens with H/D ratio of 2. The specimens were cut from a long intact sample, together with the corresponding specimens for UCS and Brazil tests. The sample was without visible fissures and the resulting specimens showed negligible variation of bulk density around 2.08 g/cm$^3$.

The cyclic tests have been carried out on saturated specimens. The end platens were rough. The specimens were anisotropically consolidated to in situ stress following radial to axial stress ratio of about 0.3. The subsequent cyclic phases are carried out in undrained conditions, with a frequency of 0.1 Hz. The results of these tests are presented in Figure 13.

The first cyclic test has been carried out with two phases of 100 cycles each, with average stress ratio of about 0.19, and the cyclic stress ratio about 0.17 in the first phase, and 0.37 and 0.33 in the second phase. The stated stress ratios are referring to the strength of the UCS specimen cut out from the same sample, assuming that for the neighboring specimens, the same apparent bulk density would result in the same compression strength. However, as a variation of the UCS strength could occur at the same bulk density (cf. Figure 11), the stress levels were cautiously chosen, so that the maximum shear stress during the cyclic phase would not exceed about 70% of the shear stress based on UCS test, in order to ensure observation of the post-cyclic shear strength. See the outlined UCS-Brazil data point in Figure 13 obtained by combining the test results on the accompanying specimens from the same sample. In the post-cyclic shear phase, the specimen exceeded the estimated shear strength.

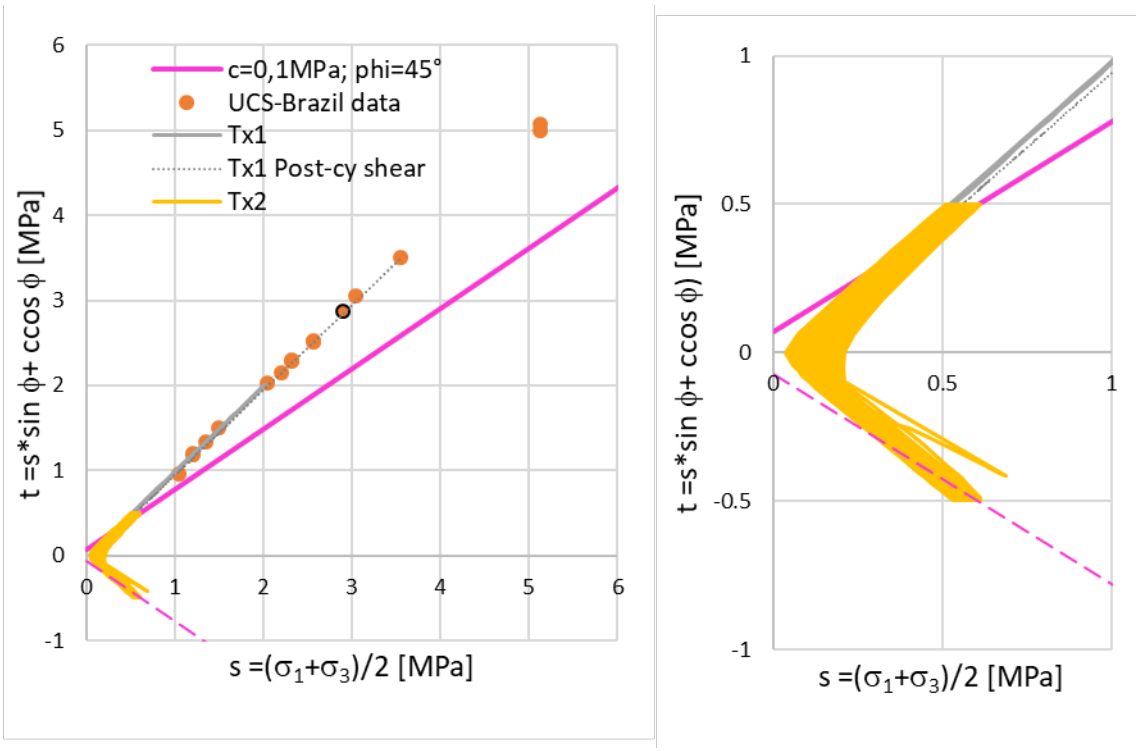


(a) (b)

**Figure 13.** Strength test results in s-t space**.** a: all strength tests. b: detail of the second cyclic test.

The second test has been carried out with the average stress ratio of 0 and the cyclic stress ratio of ~0.18. This was a maximal cyclic stress ratio that could be applied for the average stress ratio of 0, as higher ratios required backpressures beyond the equipment capability. The sample reached 37 cycles, upon which it split orthogonally to the coring direction. This is interpreted as fatigue along a plane of weakness parallel to the bedding plane. The failure incidentally occurred along the failure locus defined for friction angle of 45 degrees and c' of 100 kPa.

The cyclic testing thus indicated the following:

- The matrix material is fairly resilient to cycling in undrained conditions and upon 100 cycles at the high deviator stress, no strength reduction is observed.
- The matrix material is potentially less resilient to cycling between compression shear and extension shear. As no pre-existing fissures or variations were observed on the sample, the observed failure can also be considered as a model of fracturing/remolding of the matrix under natural conditions. This hypothesis could explain the coincidental match of the failure stress and the typical strength of the rock mass.

## 5. Commentary and discussion

The dominant orientation of large fractures anticipated based on Sigerslev quarry observations is confirmed at Stevns Klint by the site inspection. The thicknes of the upper fractured zone of the limestone is found smaller at Stevns Klint.

Careful handling of the material was exercised in order to preserve the natural state of the

gathered samples as much as possible. Considering the limitations of the current testing budget, the program for the laboratory testing on Stevns Klint is primarily designed to assess the properties of the weakest parts of the rock, i.e. focusing on the samples of induration H2. Some of the testing has been carried out on the samples with higher indurations, primarily to confirm the agreement with the existing trends.

All the data gathered on the project is in good agreement with the anticipated trends.

The specimens tested in the laboratory are hand picked to reflect the properties of the weakest encountered parts of the rock matrix and provide low estimate strengths. Except for one dented specimen, where the dent is likely caused by chipping of a fossil from the surface of the sample, the specimens tested in the laboratory were intact, without visible fractures or fissures, and very accurate geometrically.

Looking at the total UCS data set, it is observed that the variation of unconfined strength of specimens with low densities is a direct consequence of the cementation state (Figure 14). The extremely weak limestone with low bulk density found on Sjælland is not seen in the rather elaborate dataset from Malmø. The extreme strengths, possibly relating to a high opal content, seem to be more frequent in low density specimens from Malmø, whereas on Sjælland they are more often registered for densities in the range of 2.0 to 2.2 g/cm$^3$, albeit not on Stevns Klint. This is indicating that the local geological conditions govern the appearance of extreme values.

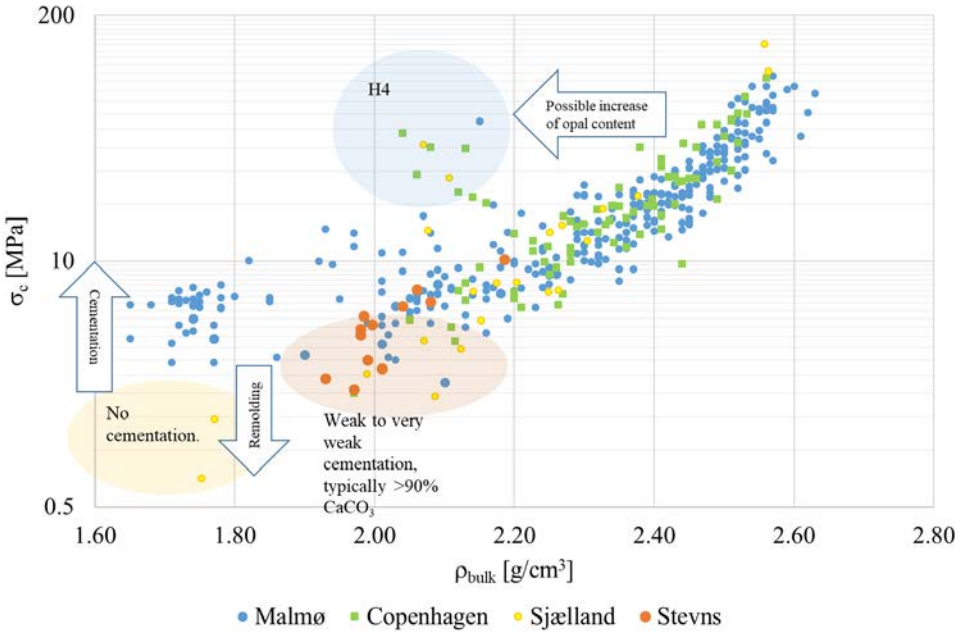


**Figure 14.** UCS database observations.

At the end, it should be also observed that the UCS tests are typically conducted parallel to the core—in a direction close to orthogonal to the bedding. Whereas the current experience and this work did not discredit isotropy of the carbonate part of the rock matrix, the strength anisotropy is a known feature of flint. This indicates that the orientation of the flint particles may influence the response of the sample and produce anisotropy, thereby increasing the scatter.

## 6. Conclusion

The existing experience and database information has been used throughout this work to identify the potential problems. The observed trends enabled formulation of the worst-case scenario for the given structure. Hereafter, it was possible to focus the investigation program towards revealing the information which was not available from the existing sources. As an illustration, no testing of high induration samples nor fractured samples was deemed necessary to establish the relations between intact and mass properties of the rock. An example of potentially critical information not available from other sources is sensitivity to freeze-thaw and to cyclic loading added in the current project.

The geotechnical information from this investigation campaign is found to fit well with the overall information available in the database. Starting from the observed features of the material at hand, the article states reflections on some of the observed responses of the Bryozoan limestone found in the database.

## Acknowledgments

The authors are grateful to Geo's project manager, Carsten Bonde, for his support throughout the project and for encouraging the preparation of this manuscript. We would exceptionally like to acknowledge Mads Robenhagen Mølgaard for modeling support throughout the project and GeoAtlas Live figures used in this paper, as well as Niels Trads for the assistance and supervision of the cyclic triaxial testing of limestone. Finally, we would like to thank Geo for the time allocated to the preparation of this work.

## Conflict of interest

All authors declare no conflicts of interest in this paper.

## References

1. Jackson PG, Steenfelt JS, Foged NN, et al. (2004) Evaluation of Bryozoan limestone properties based on in-situ and laboratory element tests. *Geotech Geophys Site Charact* 1813–1820.
2. Foged NN (2008) Rock Mass Characterisation in Limestone. Lecture presented at Dansk Geoteknisk Forening Mode nr. 2 Generalforsamling. (Danish Geotechnical Society Meeting nr. 2 General assembly.)
3. Foged NN, Hansen SL, Stabell S (2010) Developments in Rock Mass Evaluation of Limestone in Denmark. In: *Rock mechanics in the Nordic countries*, Norway: Kongberg.
4. Galsgaard J. (2014) Flint in the Danian København Limestone Formation. (Flint in the Danian Copenhagen Limestone Formation.) Available from: https://www.geo.dk/media/1951/flint-in-the-danian-koebenhavn-limestone-formation_jgalsgaard_2014.pdf
5. Jakobsen L, Foged NN, Erichsen L, et al. (2015) Face logging in Copenhagen Limestone, Denmark. *Proceedings of the XVI ECSMGE Geotechnical Engineering for Infrastructure and Development*, 2939–2944.

6. Hansen SL, Galsgaard J, Foged NN (2015) Rock mass characterization for Copenhagen Metro using face logs. SEE TUNNEL—Promoting tunnelling in SE European region, Presented at: 41st General Assembly and Congress of International Tunneling and Underground Space.
7. Katić N, Christensen HF (2014). Upscaling elastic moduli in Copenhagen Limestone. In *Rock Engineering and Rock Mechanics: Structures in and on Rock Masses: Proceedings of EUROCK 2014, ISRM European Regional Symposium*, London: Taylor & Francis Group, 235–240.
8. Katić N, Christensen HF (2015) Composite Elasticity of Copenhagen Limestone. In *Proceedings of the ISRM Regional Symposium EUROCK 2015 & 64th Geomechanics Colloquium—Future Development of Rock Mechanics*, Salzburg: Austrian Society for Geomechanics, 451–456.
9. Vangkilde-Pedersen T, Mielby S, Jakobsen PR, et al. (2011) *Kortlægning af kalkmagasiner*. GEUS. Geo-vejledning 8. De nationale geologiske undersøgelser for Danmark og Grønland. Ministeriet for klima og energy. (*Mapping of limestone reservoirs.* GEUS. Geo-guidance 8. National geological investigations for Denmark and Greenland. Ministry of climate and energy.) Available from: gk.geus.info/xpdf/geovejledning_8_kalk_final_net.pdf.
10. Bjerager M, Surlyk F (2007) Danian Cool-Water Bryozoan Mounds at Stevns Klint, Denmark–A New Class of Non-Cemented Skeletal Mounds. *J Sediment Res* 77:634–660.
11. Japsen P, Bidstrup T, Lidmar-Berström K (2002) Neogene uplift and erosion of southern Scandinavia induced by the rise of the South Swedish Dome. *Geol Soc* 196: 183–207.
12. Andersen TB, Møgaard MR (2018) Copenhagen Area Overview of the geological conditions in the Copenhagen area and surrounding areas. GeoAtlas Live Documentation. Report 1. Available from: http://wgn.geo.dk/geodata/modeldokumentation/Copenhagen%20_25m_2018-07-12.pdf
13. Olsen H, Nielsen UT (2002) Logstratigrafisk inddeling af kalken I Københavns-området. In Frederiksen JK, Eriksen FS, Hansen HK, et al., editors. Ingeniørgeologiske forhold i København. Dgf-Bulletin 19, Danish Geotechnical Society. (Logstratigraphical division of limestone in Copenhagen Area. In Frederiksen JK, Eriksen FS, Hansen HK, et al., editors. Engineering-geological conditions in Copenhagen. Dgf-Bulletin 19, Danish Geotechnical Society.)
14. Damholt T, Surlyk F (2012) *Nomination of Stevns Klint for inclusion in the World Heritage List*. Østsjællands Museum. Pedersen AS (2011) Rockfalls at Stevns Klint. Landslide hazard assessment based on photogrametrical supported geological analysis of the limestone cliff Stevns Klint in eastern Denmark. *Danmarks og Grønlands Geologiske Undersøgelse Rapport 2011/93* (*Danmark's and Greenland's Geological Investigaton Report 2011/93*). Available from: https://whc.unesco.org/uploads/nominations/1416.pdf.
15. Mortensen N, Hansen HK, Hansen PB (1999) Malmö Citytunneln. Rock Mechanical Description. Limestone. Malmö (SE). 32p. Report 1, 22 March 1999, Revision 1. DGI job No. 155 16092. Geo archive.
16. Jørgensen NO (1975) Mg/Sr distribution and diagenesis of Maastrichtian white chalk and Danian bryozoan limestone from Jylland, Denmark. *Bull Geol Soc Den* 24: 299–325.
17. Rosenbom A, Jakobsen PR (2000) Kalk, Sprækker og Termografi. *Geol Nyt fra GEUS* 3: 1–8. (Chalk, Fractures and Thermography. *Geol News From GEUS* 3: 1–8.)
18. Surlyk F, Damholt T, Bjerager M (2006) *Stevns Klint, Denmark: uppermost Maastrichtian chalk, Cretaceous-Tertiary boundary, and lower Danian bryozoan mound complex*, Geological Society of Denmark, 54: 1–48.

19. Hoek E, Carter TG, Diedrichs MS (2013) Quantification of the Geological Strength Index Chart. *47th US Rock Mechanics/Geomechanics Symposium*, 1757–1764.
20. Eberli GP, Beachle TG, Anselmetti FS, et al. (2003) Factors controlling elastic properties in carbonate sediments and rocks. *Lead Edge* 22: 654–660.
21. Brigaud B, Vincent B, Durlet C, et al. (2010) Acoustic properties of ancient shallow-marine carbonates: effects of depositional environments and diagenetic processes (Middle Jurassic, Paris basin, France). *J Sediment Res* 80:791–807.
22. Bergdahl U, Steenfelt JS (1994) *Digest report on strength and deformation properties of Copenhagen limestone*, Swedish Geotechnical Institute/Danish Geotechnical Institute, 67.


AIMS Press